Article

Sugarcane Bagasse Ash as an Alternative Source of Silicon Dioxide in Sodium Silicate Synthesis

Jesús Abraham Pérez Casas , Anabel Álvarez Mendez , Juan Jacobo Ruiz Valdés , Salomé De La Parra , Antonio A. Zaldivar-Cadena , David López Pérez , Astrid Iriana Sánchez Vázquez *

Posted Date: 30 June 2023

doi: 10.20944/preprints202306.2233.v1

Keywords: Sugarcane bagasse ash; solid state reaction; sodium silicate

Preprints (www.preprints.org) | NOT PEER-REVIEWED | Posted: 30 June 2023 doi:10.20944/preprints202306.2233.v1

Article

Sugarcane Bagasse Ash as an Alternative Source of Silicon Dioxide in Sodium Silicate Synthesis

Jesús A. Pérez-Casas[1], Antonio A. Zaldívar-Cadena[2], Anabel Álvarez-Mendez[1], Juan Jacobo Ruiz-Valdés[1], Salomé M. de la Parra-Arciniega[1], David C. López-Pérez[2] and Astrid I. Sánchez-Vázquez[1]*

[1] Universidad Autónoma de Nuevo León, Facultad de Ciencias Químicas, Avenida Pedro de Alba s/n, San Nicolás de los Garza 66455, N.L., Mexico; jesus.perezcs@uanl.edu.mx (J.A.P-C); anabel.alvarezmn@uanl.edu.mx (A.Á.-M.); juan.ruizv@uanl.mx (J.J.R.-V.); smdlp@yahoo.com (S.M.d.l.P.-A.); asirisan@yahoo.com.mx (A.I.S.-V.)

[2] Universidad Autónoma de Nuevo León, Facultad de Ingeniería Civil, Avenida Universidad s/n, San Nicolás de los Garza 66455, N.L., Mexico; azaldiva70@hotmail.com (A.A.Z-C.), david.lopezpr@uanl.edu.mx (D.C.L.-P.)

* Correspondence: astrid.sanchezvz@uanl.edu.mx

Abstract: To reduce environmental impacts from sodium silicate synthesis it was suggested the use of sugarcane bagasse ash (SCBA) as a source of silicon dioxide and sodium carbonate using the ceramic method. Although the production of sodium silicate is carried out on a large scale, it should be noted that its process requires temperatures above 1000 °C or the use of highly corrosive agents such as sodium hydroxide and chlorine gas used to neutralize the remaining sodium hydroxide. In the present work, the synthesis temperatures were reduced to 800 °C with a reaction time of 3 hours by pressing equimolar mixtures of previously purified SCBA and sodium carbonate, then heat treatment was carried out under the indicated conditions. The resulting materials were analyzed by Fourier transform infrared spectroscopy (FTIR) and X-ray diffraction (XRD). Among the crystalline phases, calcium disodium silicate was identified, in addition to sodium silicate, so it was inferred that the other components of the ash can interfere with the synthesis of silicate. Therefore, to obtain the highest composition of sodium silicate, a leaching treatment of the SCBA is required.

Keywords: sugarcane bagasse ash; solid state reaction; sodium silicate

---

1. Introduction

As the main residue of the sugar industry, sugarcane bagasse ash (SCBA) has the disadvantage of an accumulation derived from its low demand. This residue is currently used as fertilizer in sugarcane plantations, however, only in Mexico, approximately 500 kt of this waste is produced annually. SCBA is not merely an inorganic residue, since it retains a carbon content in its composition, so its accumulation leads to bad environmental practices such as burning the ash in the open. Considering the high concentration of SiO_2 in SCBA, its use has been proposed in the synthesis of ceramic materials, mainly light blocks, tiles, and glass-ceramics, however, the problem of increased porosity in the materials arises, which is explained by the remaining carbon which generates CO_2 during the synthesis of the materials. This porosity decreases the mechanical properties and in turn increases the absorption of water, which, in environments where the temperature reaches ranges lower than the freezing point, it can cause the material to collapse [1,2].

In the case of glasses and glass ceramics, performance problems are caused due to replacing the SCBA with alkaline carbonates that act as fluxing agents, the decomposition of said carbonates and the burning of the remaining carbon in the ash promote the generation of CO_2, and therefore pores in the vitreous material. The pores or bubbles in the glass material can decrease if the temperature is increased enough so that the viscosity of the glass allows the flow of gas, but this implies a high energy consumption [3–5].

Instead to synthetize glass with SCBA, there are other products with diverse applications such like sodium silicate which can be used as binder in concrete, synthesis of aerogels for water remediation, raw material in cosmetic and paper industries, in synthesis of high-performance magnets and the synthesis of anticorrosive coatings for metals and hydrophobic coatings for ceramics [6–10]. With the drawback that SCBA does have a diverse and complex composition, its amount of SiO_2 is not always the same and its other components can interfere with the synthesis. However, unlike the synthesis of glasses, Na_2SiO_3 requires lower temperatures for its synthesis regardless of whether Na_2CO_3 or Na_2O are used as reagents.

The common process in the synthesis of sodium silicate is the thermochemical method, which consists of the reaction of silica with sodium hydroxide (NaOH) at temperatures above 300 °C[11]. However, to isolate SiO_2 from ashes, the use of HNO_3 has been reported [12], suggesting an impact on both principles 4 and 6 of green chemistry[13]. Besides since the synthesis temperature is lower than the temperature used in other methods, there are some inconveniences with the use of NaOH. The first one is that it is a highly corrosive agent which can damage steel alloys [14], the second is that not all sodium hydroxide reacts during synthesis, so it must be neutralized using chlorine gas and finally the use of NaOH represents significant damage to the environment and human health as reported by Ingrao [15].

In this work, the use of the ceramic method is proposed which only impact principle 6 of green chemistry. For the synthesis, pellets were prepared with SCBA together with sodium carbonate in a 1: 1 molar ratio between silicon oxide and sodium oxide. The use of a carbonate instead an oxide has some implications such as stoichiometric calculations, the increase of reaction time because the carbonate must be decomposed previous the reaction and the subsequent release of CO_2 to the atmosphere because of decomposition (Equation 1). Since the applications of sodium silicate are focused on the solution[9,10,16], the increase in porosity and the mechanical properties of the material obtained are not relevant, so in this case, the disadvantages presented using SCBA, have no relevant impact on the result. Since the composition of the ash varies according to geographical location, a characterization is necessary prior to its use. In addition to this, as it was mentioned before, traces of carbon and other elements were found in the ash, so it was necessary a purification process.

$$Na_2CO_3 \rightarrow Na_2O + CO_2 \qquad (1)$$

2. Materials and methods

2.1. Characterization of Sugarcane bagasse ash

The SCBA was obtained from the Xicotencatl sugar mill, located at the south of Tamaulipas, México. Besides, reagent-grade Sigma Aldrich sodium carbonate was used for the synthesis.

The SCBA was analyzed to quantify its content of volatile material as reported in the previous work[5]. After its analysis, the ash was calcinated following the procedure reported by Sultana et al.[17] and subsequently ground by hand in an agate mortar to a homogeneous mesh size at 150 microns to maximize the contact area between the ash and Na_2CO_3. The grounded ash was analyzed by XRD (Bruker D2 Phaser) to identify the predominant crystalline phase of SiO_2, and X-ray fluorescence (Panalytical Epsilon 3) to assess the amount of silicon oxide and proceed to make the corresponding stoichiometric calculations to prepare the pellets with 1:1 and 1:2 SiO_2-Na_2O molar ratio, the mixture of reagents was carried out in the same way in an agate mortar to reduce the loss of material in the mills, especially considering the hygroscopic property of Na_2CO_3, which makes it easier for it to adhere to the walls of the mill.. Considering that there is more than one type of sodium silicate structure, and this varies depending on the molar ratio that reactive oxides maintain, according to the reaction (Equation 2):

$$XNa_2O + SiO_2 \rightarrow Na_{2x}SiO_{2+x} \qquad (2)$$

As there are other elements in the SCBA, a leaching treatment was necessary. For this process, the ash was leached with 2% wt. citric acid for 2h at 60 °C, according to Yahya et al. [18] work, and analyzed by XRF after the leaching process, the impact of this process is reported in the results and discussions section.

doi:10.20944/preprints202306.2233.v1

2.2. Sample preparation

For the preparation of the pellets, 1 gram of mixture of SCBA and Na_2CO_3 was pressed in a Craver press apparatus with a 10 mm dice, to obtain the working pressure, a design of experiments was made for assessing pressures of 2, 6, and 10 tons and times of 5, 7.5, and 10 min, measuring as a response the integrity of the obtained tablets. Since the measured response is not numerical, the best conditions were those that required less pressure, and less time and allowed the tablet to remain intact.

Once the pellets were obtained, the synthesis was carried out in a Carbolite 1300 W oven, at a temperature of 800 °C for 3 hours, maintaining the pellets inside the furnace chamber up to room temperature to allow crystallization to continue in a controlled way.

2.3. Sodium silicate characterization

The material obtained from pellets with a 1:1 molar ratio was grounded into a fine powder; it was characterized by X-ray diffraction in a Bruker D2 Phaser using Match 3! to identify the crystalline phases and a Rietveld method to quantify the crystalline phases ratio. While samples with 1:2 molar ratio were analyzed by FTIR in a Bruker Alpha II spectrometer to determine the presence of reagents in the obtained material.

3. Results and discussions

As it was reported in our previous work[19], according to the elemental analysis before and after the calcination, a decrease of a %wt/wt. from 15.86 to 0.12% of carbon content was observed, meaning an almost total elimination. From the XRF analysis (Table 1) it is possible to identify the main inorganic components in SCBA, in which, silicon oxide is the main component and calcium stands out as the second major component. The high concentration of calcium becomes relevant considering that the ionic radii of Ca^{2+} and Na^{+} are very similar (1.14 and 1.16 Å respectively), which may imply competition in the selectivity on crystallization reactions of silicates [20]. Citric acid leaching process was suggested to reduce calcium concentration from ash.

Table 1. SCBA composition after calcination and purification.

Compound	%wt/wt.	Leached ash %wt/wt.
Na_2O	0.48	0.00
MgO	0.92	0.30
Al_2O_3	2.21	1.70
SiO_2	70.85	78.61
P_2O_5	1.15	1.28
SO_3	1.46	0.25
K_2O	4.34	5.61
CaO	12.73	7.45
TiO_2	0.44	0.47
MnO	0.13	0.11
Fe_2O_3	4.82	4.05
CuO	0.03	0.02
ZnO	0.06	0.03
SrO	0.13	0.05
ZrO_2	0.02	0.01
Ag_2O	0.18	0.06
BaO	0.04	0.00
Total	100	100

doi:10.20944/preprints202306.2233.v1

In the pressure test of the pellets of SCBA and sodium carbonate, with higher time and pressure, the pellets become fragile. This behavior can be explained due to the increase in pressure, as the pressure between the powder and the dice is greater, the friction between the pellet and the walls of the dice becomes greater, culminating in the destruction of the pellet during the procedure to release it from the dice [21]. Thus, the best result corresponds to a pressure of two tons which is the lowest pressure tested and a time of 5 minutes. At these conditions the stress over the pellet was lowest and the sample was easily removed from the dice.

Figure 1 shows the diffractogram corresponding to the SCBA, where quartz is observed as the main crystalline phase, this result is different from that reported by Sultana[17], where at a higher temperature the predominant crystalline phase in the SCBA was reported as cristobalite after a heat treatment at 800 °C for 2 hours. Even so, it could be inferred that the cristobalite formed during calcination reacted with CaO present in the SCBA forming the calcium silicate as it's observed in the diffractogram. Quartz has an interstitial space in its cell of approximately 3 Å similar to interstitial space of cristobalite [22]. 3 Å is considered as sufficient distance for the sodium and calcium ions to be able to diffuse through the silicon dioxide crystalline cell, since calcium silicate appears as a secondary phase, it is possible to suggest that other elements react with the silicon dioxide of the ash besides sodium oxide.

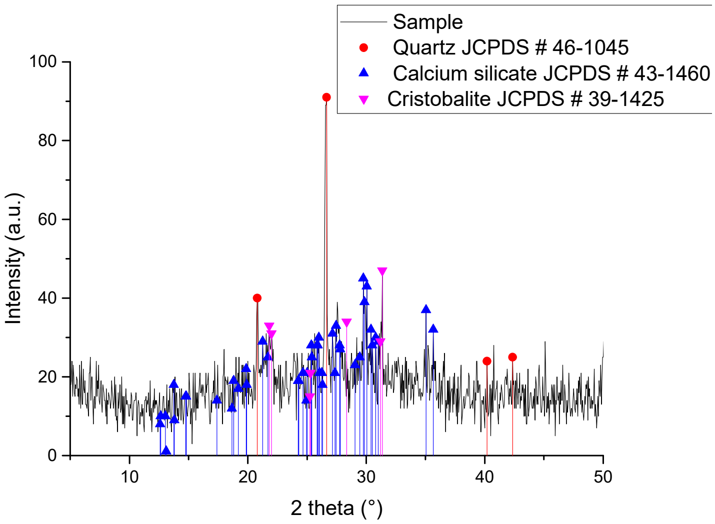

Figure 1. XRD of SCBA after the calcination at 900 °C.

Considering that the reaction was carried out in solid state, the way it occurs is through a diffusion mechanism between the crystalline cells of silicon dioxide and the other reactant oxides. If the diameter is similar for both ions (sodium and calcium), a kind of competition can be generated to occupy the interstices in the silicon oxide network. Thus, allowing the generation of both sodium silicate and sodium-calcium silicate, as shown in Figure 2 [23].

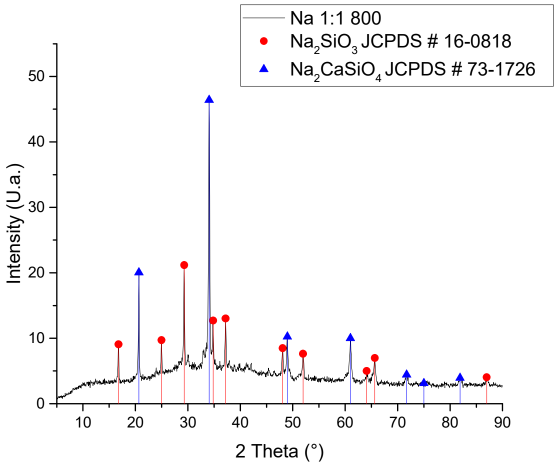

Figure 2. XRD for the sodium silicate synthesized with non-leached ash.

It is worth mentioning that even though the presence of disodium calcium silicate is an inconvenience for this project, this material is identified as a bioceramic with important applications in bone regeneration and localized drug delivery [24]. To increase the ratio of sodium silicate in the synthesized material, samples were synthesized in a molar ratio of 1:2 SiO_2-Na_2O, but a clear lack of reaction was observed, in the FTIR spectrum of Figure 3. The signal at 1500 cm^{-1} is characteristic of the bond C=O present in carbonate, the lack of reaction can be explained due to the thermal stability of the internal carbonate, requiring a higher temperature or a longer synthesis time considering the heat transfer phenomena. Even so, the presence of the signal at 950 cm^{-1} corresponds to the Na-O-Si bond, suggesting the presence of a chemical reaction[25]. About the signals between the range of 500 to 880 cm^{-1} correspond to the bending of the C=O bond outside (600 to 700 cm^{-1}) and inside the plane (840 to 880 cm^{-1}), while the signal around 1050 to 1100 cm^{-1} it is characteristic of the stretching of the Si-O bond [25,26]. The most important signals are those corresponding to 1500 and 950 cm^{-1}, because although the signal at 1050-1100 cm^{-1} also corresponds to the stretching of the Si-O bond, it can refer to both the presence of SiO_2 like some silicate. The signal at 1500 cm^{-1} is typical of the C=O bond while the signals at a lower wavenumber may correspond to other bonds such as the bending of the Si-O bond [27].

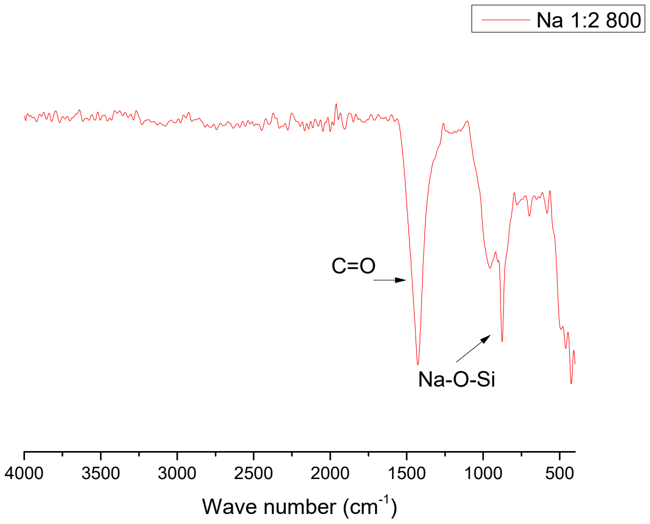

Figure 3. FTIR of sodium silicate synthesized with a molar ratio of 1:2 SiO_2-Na_2O.

As per the results of the synthesis developed with the untreated ash (Figure 2), the use of a purification technique for the ash was proposed, carrying out a leaching process with citric acid at a concentration of 2% wt/v at a temperature of 60 °C for 2h[19]. Citric acid, unlike the nitric acid used to extract SiO_2 from the ashes, is a weak acid with a low environmental impact. In this way, the calcium concentration was reduced, achieving a reduction of approximately 5% of the calcium in the ash (Table 1), and obtaining a purer sodium silicate as observed in the diffractogram of Figure 4.

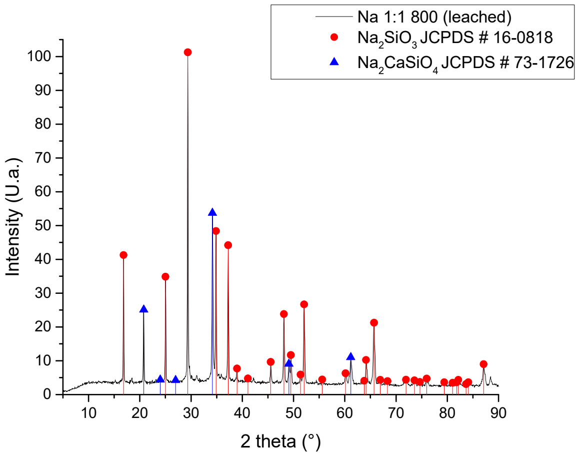

Figure 4. XRD of sodium silicate synthesized with leached ash.

With sodium silicate as the main crystalline phase, it is possible to separate both silicates considering that disodium calcium silicate is a water-insoluble compound, so a decantation and filtering process would allow obtaining a solution of sodium silicate. Unlike Vinai's work [11], which used the thermochemical method with NaOH, the results obtained in this research present a single crystalline phase of sodium silicate Na_2SiO_3, and in Vinai's report, there are signs corresponding to three polymorphs of sodium silicate. The importance of the homogeneity of the crystalline phases lies in the fact that, in the case of sodium silicate, each crystalline phase has different applications and properties.

Before presenting the results of the Rietveld refinement, it should be considered, in addition to the results presented, that the XRD technique has a detection limit of 5%, so the presence of other crystalline phases after heat treatment is possible, such as a possible potassium silicate, since observing what is presented in Table 1 as well as the melting temperature of potassium oxide (740 °C) it is possible that a synthesis process occurred in parallel.

The Rietveld refinement was carried out starting from the results obtained from the XRD analysis by means of the software "Match3!" and making use of the Maud software. For this process, in addition to analyzing the results of the synthesis after 3 hours of reaction, the behavior of the reaction was examined from 0.5 to 3 hours. Figure 5 shows the diffractograms corresponding to this analysis.

doi:10.20944/preprints202306.2233.v1

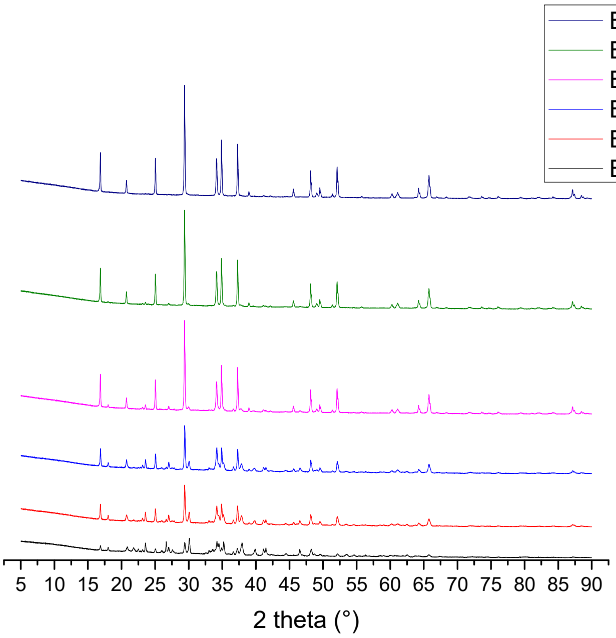

Figure 5. Crystallinity of the sample at different reaction time.

From Figure 5, letter B represents the serial experiments while 800 is the synthesis temperature and the last numbers the reaction represented time from 0.5 to 3 hours. It is possible to observe how starting from a diffractogram with a considerable noise content corresponding to amorphous signals coming from the ash, the intensity of the signals becomes more and more intense until there are no significant differences between 2.5 and 3 hours of elapsed time, for The Rietveld refinement identified the crystalline phases presented in Table 2. Unlike the other diffractograms presented, the CIF identifications were used instead of JCPDS because the Maud software only admitted the crystallographic sheets corresponding to the CIF files.

Table 2. Crystalline phases identified for Rietveld refinement.

Phase	CIF
Na_2CO_3	96-210-6298
Na_2SiO_3	96-231-0859
Na_2CaSiO_4	96-101-0112
Quartz	96-901-5023
SiO_2 (no polymorph identified)	96-900-6299
NaO_2	96-412-4632
Cristobalite	96-901-4487

Unlike the other diffractograms presented, the CIF identifications were used instead of JCPDS because the Maud software only admitted the crystallographic sheets corresponding to the CIF files. However, the identifications correspond to the same phases identified with their respective JCPDS number. Table 3 shows the compositions corresponding to the crystalline phases identified at each reaction time. For the construction of Table 3, the different SiO_2 polymorphs were integrated into one because when analyzing them individually, confusing information is generated due to the constant change between polymorphs due to temperature, the same behavior studied by Sultana [17].

Table 3. Composition of the sample taken at different reaction time.

Sample	*SiO_2*	*Na_2CO_3*	*NaO_2*	*Na_2SiO_3*	*Na_2CaSiO_4*
B0.5	0.42	0.31	0.10	0.12	0.045
B1.0	0.39	0.27	0.00	0.27	0.072

B1.5	0.34	0.27	0.00	0.28	0.10
B2.0	0.23	0.20	0.00	0.44	0.13
B2.5	0.24	0.00	0.00	0.62	0.14
B3.0	0.00	0.00	0.00	0.81	0.19

The presence of sodium superoxide in the first half hour of reaction, despite being an unstable crystalline phase under reaction conditions, has been reported as a common intermediate in the formation of Na_2O from Na_2CO_3, according to what was reported by Maheshwari [28], even thus, this intermediate disappears immediately to produce Na_2O. After 2.5 hours of reaction, the presence of SiO_2 is still observed, which disappears after half an hour, since the amount of unreacted calcium present is unknown, it is hypothesized that part of the Na_2CaSiO_4 decomposes to give rise to Na_2SiO_3 while that the rest of the SiO_2 continues to react with the calcium present in the ash. This hypothesis is unfounded considering that if Na_2CaSiO_4 decomposed to produce Na_2SiO_3, the amount of Na_2SiO_4 would be less than the 19% reported at the end of the experiment.

4. Conclusions

Sugarcane bagasse ash can be used in the synthesis of sodium silicate at a lower temperature (800 °C) than that used in the usual synthesis of this compound (1000 - 1200 °C). However, it is necessary to carry out a purification treatment by means of citric acid leaching to reduce the calcium concentration and thus decreasing the sodium-calcium silicate concentration.

Increasing the sodium carbonate concentration did not benefit the obtaining of sodium silicate due to the high thermal stability of sodium carbonate inside the pellet, which was the reason to use a 1:1 molar ratio between SiO_2 and Na_2O. Carrying out the synthesis with SCBA treated with citric acid resulted in obtaining Na_2SiO_3 as the main product, reaching up to 81% of the composition of the final product. to purify the product obtained it is possible to make use of the insolubility of Na_2CaSiO_4.

Acknowledgments: The authors acknowledge the CONACyT for the funding of the project and to the Universidad Autónoma de Nuevo León for the infrastructure to make possible the experiments; and finally, Ángela Lizeth Cantú Leal for her help during the first steps of the experiments.

References

1. S.M.S. Kazmi, S. Abbas, M.A. Saleem, M.J. Munir, A. Khitab, Manufacturing of sustainable clay bricks: Utilization of waste sugarcane bagasse and rice husk ashes, Constr Build Mater. 120 (2016) 29–41. https://doi.org/10.1016/j.conbuildmat.2016.05.084.
2. J. James, P.K. Pandian, A Short Review on the Valorisation of Sugarcane Bagasse Ash in the Manufacture of Stabilized / Sintered Earth Blocks and Tiles, Advances in Materials Science and Engineering. 2017 (2017) 15.
3. S.R. Teixeira, A.E. Souza, C.L. Carvalho, V.C.S. Reynoso, M. Romero, J.M. Rincón, Characterization of a wollastonite glass-ceramic material prepared using sugar cane bagasse ash (SCBA) as one of the raw materials, Mater Charact. 98 (2014) 209–214. https://doi.org/10.1016/j.matchar.2014.11.003.
4. A.E. Souza, S.R. Teixeira, G.T.A. Santos, F.B. Costa, E. Longo, Reuse of sugarcane bagasse ash (SCBA) to produce ceramic materials, J Environ Manage. 92 (2011) 2774–2780. https://doi.org/10.1016/j.jenvman.2011.06.020.
5. j. Pérez, uso de la ceniza de bagazo de caña de azúcar como fuente de sio2 para síntesis de materiales vitrocerámicos con aplicaciones en la construcción, Universidad Autónoma de Nuevo León, 2018.
6. S.A. Bernal, J.L. Provis, V. Rose, R. Mejía De Gutierrez, Evolution of binder structure in sodium silicate-activated slag-metakaolin blends, Cem Concr Compos. 33 (2011) 46–54. https://doi.org/10.1016/j.cemconcomp.2010.09.004.
7. Sodium and Potassium silicates Versatile compounds for your applications, (2004) 16.
8. Z. Mazrouei-Sebdani, S. Salimian, A. Khoddami, F. Shams-Ghahfarokhi, Sodium silicate based aerogel for absorbing oil from water: The impact of surface energy on the oil/water separation, Mater Res Express. 6 (2019). https://doi.org/10.1088/2053-1591/ab1eed.
9. R. Farid, K. Rajan, D.K. Sarkar, Surface & Coatings Technology Enhanced corrosion protection of aluminum by ultrasonically dip coated sodium silicate thin fi lms, Surf Coat Technol. 374 (2019) 355–361. https://doi.org/10.1016/j.surfcoat.2019.05.082.

10. W. Liu, W. Xi, R. Hu, M. Yue, Y. Yin, J. Guo, Preparation and characterization of sodium silicate / epoxy resin composite bonded Nd-Fe-B magnets with high performance *, Journal of Rare Earths. (2019). https://doi.org/10.1016/j.jre.2019.03.012.
11. R. Vinai, M. Soutsos, Cement and Concrete Research Production of sodium silicate powder from waste glass cullet for alkali activation of alternative binders, Cem Concr Res. 116 (2019) 45–56. https://doi.org/10.1016/j.cemconres.2018.11.008.
12. Q. Alam, Y. Hendrix, L. Thijs, A. Lazaro, K. Schollbach, H.J.H. Brouwers, Novel low temperature synthesis of sodium silicate and ordered mesoporous silica from incineration bottom ash, J Clean Prod. 211 (2019) 874–883. https://doi.org/10.1016/j.jclepro.2018.11.173.
13. N. Ahmad, F. Ahmad, Green Chemistry: Principle and its Application, in: 2nd International Conference on Advancement in Engineering, Applied Science and Management, 2017. https://www.researchgate.net/publication/322078077.
14. M. Abdallah, M.M. Salem, I.A. Zaafarany, A. Fawzy, A.A. Abdel Fattah, Corrosion performance of stainless steel and nickel alloys in aqueous sodium hydroxide as revealed from cyclic voltammetry and potentiodynamic anodic polarization, Oriental Journal of Chemistry. 33 (2017) 2875–2883. https://doi.org/10.13005/ojc/330621.
15. C. Ingrao, C. Saja, P. Primerano, Application of Life Cycle Assessment to chemical recycling of post-use glass containers on the laboratory scale towards circular economy implementation, J Clean Prod. 307 (2021). https://doi.org/10.1016/j.jclepro.2021.127319.
16. U. Zulfiqar, M. Awais, S.Z. Hussain, I. Hussain, S.W. Husain, T. Subhani, Durable and self-healing superhydrophobic surfaces for building materials, Mater Lett. 192 (2017) 56–59. https://doi.org/10.1016/j.matlet.2017.01.070.
17. M.S. Sultana, M.A. Rahman, M.N. Zaman, A.N. Ahmed, Influence of Calcination on Different Properties of Sugarcane Bagasse and Waste Ash, Journal of Scientific Research. 7 (2015) 151–157.
18. A.A. Yahya, N. Ali, N.L. Mohd Kamal, S. Shahidan, S. Beddu, M.F. Nuruddin, N. Shafiq, Reducing Heavy Metal Element from Coal Bottom Ash by Using Citric Acid Leaching Treatment, MATEC Web of Conferences. 103 (2017) 0–6. https://doi.org/10.1051/matecconf/201710301004.
19. J.A. Pérez-Casas, A.A. Zaldívar-Cadena, A. Álvarez-Mendez, J.J. Ruiz-Valdés, S.M. de la Parra-Arciniega, A.I. Sánchez-Vázquez, Synthesis of Silica Particles from Sugarcane Bagasse Ash for Its Application in Hydrophobic Coatings, Materials Proceedings. 2 (2020) 4. https://doi.org/10.3390/ciwc2020-06830.
20. Teresia. Möller, Selective crystalline inorganic materials as ion exchangers in the treatment of nuclear waste solutions, Academic Dissertation, Faculty of Science of the University of Helsinki, 2002.
21. W. Stelte, J.K. Holm, A.R. Sanadi, S. Barsberg, J. Ahrenfeldt, U.B. Henriksen, Fuel pellets from biomass: The importance of the pelletizing pressure and its dependency on the processing conditions, Fuel. 90 (2011) 3285–3290. https://doi.org/10.1016/j.fuel.2011.05.011.
22. K.J. Lin, H. Ding, M.J. Demkowicz, Formation, migration, and clustering energies of interstitial He in α-quartz and β-cristobalite, Journal of Nuclear Materials. 479 (2016) 224–231. https://doi.org/10.1016/j.jnucmat.2016.06.049.
23. D.R. Askeland, P. Fulay, Ciencia e ingeniería de materiales, (2011) 197–247.
24. P.M. Reddy, R. Lakshmi, F.P. Dass, S. Sasikumar, Synthesis, characterization and formulation of sodium calcium silicate bioceramic for drug delivery applications, Science and Engineering of Composite Materials. 23 (2016) 375–380. https://doi.org/10.1515/secm-2014-0057.
25. E.F. Medvedev, A.S. Komarevskaya, IR spectroscopic study of the phase composition for sodium silicate synthesized in aqueous medium, Glass and Ceramics. 64 (2007) 7–11. https://doi.org/https://doi.org/10.1007/s10717-007-0002-y.
26. E.S. Rufino, E.E.C. Monteiro, Characterisation of lithium and sodium salts of poly(methacrylic acid) by FTIR and thermal analyses, n.d.
27. L. Vidal, E. Joussein, M. Colas, J. Cornette, J. Sanz, I. Sobrados, J.L. Gelet, J. Absi, S. Rossignol, Controlling the reactivity of silicate solutions: A FTIR, Raman and NMR study, Colloids Surf A Physicochem Eng Asp. 503 (2016) 101–109. https://doi.org/10.1016/j.colsurfa.2016.05.039.
28. A. Maheshwari, H.D. Wiemhöfer, Augmentation of grain boundary conductivity in Ca2+ doped ceria-carbonate-composite, Acta Mater. 103 (2016) 361–369. https://doi.org/10.1016/j.actamat.2015.10.024.